Original Article

Available online at www.bpasjournals.com

Sustainable Electric Vehicle Design with Integrated Fuel Cell, Photovoltaic, and ANN-Based Model Predictive Control

G. Divya¹, Dr. Venkata Padmavathi S²

¹Ph.D Scholar, GITAM School of Technology, GITAM Deemed to be University, Hyderabad, Telangana; Assistant Professor / EEE, CVR College of Engineering, Hyderabad, Telangana

²Assistant Professor /EEE, GITAM School of Technology, GITAM Deemed to be University, Hyderabad, Telangana

How to cite this article: G. Divya, Venkata Padmavathi S (2024) Sustainable Electric Vehicle Design with Integrated Fuel Cell, Photovoltaic, and ANN-Based Model Predictive Control. *Library Progress International*, 44(3) 17403-17423.

Abstract

This paper presents a new Electric Vehicle (EV) system that combines a fuel cell, electrolyzer, onboard PV cell, and a quadratic bidirectional buck-boost converter. The system is managed by Model Predictive Control (MPC) with support from an Artificial Neural Network (ANN). The PV cell enhances the fuel cell's power output during operation and, during idle periods, powers the electrolyzer to produce hydrogen for storage. This stored hydrogen is used to fuel the vehicle, improving its energy efficiency and reducing reliance on traditional fuel sources. A quadratic bidirectional buck-boost converter is used to control voltage, improving power management between the motor and energy sources. This ensures efficient execution even when fluctuating irradiance and vehicle speeds vary. An enhanced Maximum Power Point Tracking (MPPT) algorithm, utilizing an incremental conductance method, is used to maximize energy extraction from the PV system. Meanwhile, the converter's dualloop control, featuring outer voltage and inner current control, ensures a stable DC output for motor operation. The vehicle drive system directs an indirect vector-controlled induction motor, which is set by the ANN-based MPC. This system employs a novel predictive torque control strategy that eliminates the need for weighting factors, simplifying the control process while improving motor speed regulation. Additionally, an ANN s used to accurately predict motor speed based on real-time stator current data, ensuring optimal performance and system stability. Simulations conducted in MATLAB/SIMULINK evaluate the system's performance under varying solar irradiance and speed conditions. The results determine the feasible of the proposed EV configuration to enhance energy efficiency, improve power quality, and provide a more sustainable and economically viable solution for electric vehicles by integrating renewable energy sources with advanced control techniques.

Keywords: - Electric Vehicle (EV) Configuration, Artificial Neural Network (ANN), Model Predictive Control (MPC), Photovoltaic (PV) System, Quadratic Bidirectional Buck-Boost Converter, Maximum Power Point Tracking (MPPT)

1. Introduction

The growing concerns over environmental sustainability and the reduction of fossil fuel reserves have accelerated the transition towards alternative energy sources. Among the various strategies adopted, EVs have become a practical solution for reducing greenhouse gas emissions and advancing cleaner transportation [1]. EVs not only offer a reduction in air pollution but also present an opportunity for energy diversification by integrating renewable energy sources (RES) as solar and hydrogen fuel cells. EVs are not a new idea, but their development has rapidly advanced to improve in battery technology and power electronics. Traditionally, EVs rely on batteries as their primary energy storage system, but the limitations associated with battery capacity, long charging times, and degradation over repeated cycles have led to the exploration of hybrid configurations [2]. In this context, integrating RES as PV systems and hydrogen fuel cells into EV designs presents a promising approach to overcoming the limitations of conventional battery-based EVs.

Fuel cells offer the advantage of clean energy generation, as they convert hydrogen into electricity with water as the only byproduct. This makes fuel cells an attractive solution for long-distance travel and continuous energy supply. On the other hand, PV cells provide a renewable source of energy, which can be directly harvested from sunlight, further reducing the vehicle's reliance on the grid for charging. The hybridization of these energy sources can significantly enhance the overall efficiency and sustainability of the EV, particularly when combined with an

intelligent control system like ANN-based MPC [3].

A key challenge in developing EVs is managing energy effectively. EVs require efficient control of multiple energy sources, including batteries, PV cells, and fuel cells, to optimize the vehicle's performance. A robust energy management system must balance the power output from each source in response to varying load conditions and ensure a seamless transition between them [4]. This requires advanced control strategies that can adapt to changes in environmental factors as solar irradiance, vehicle speed, and battery state-of-charge.

Conventional control methods, like Proportional-Integral-Derivative (PID) controllers and linear predictive control systems, often fall short in addressing the complexities of hybrid energy systems due to their limited adaptability to nonlinear dynamics and varying operating conditions [5]. Therefore, incorporating intelligent control systems such as Artificial Neural Networks (ANN) offers a promising solution for overcoming these limitations [6].

Another significant challenge is the efficient conversion and storage of energy. Fuel cells and PV systems work at different voltage levels, so power electronic converters are used to control the voltage and current for the vehicle's motor and battery. A key component in the proposed EV configuration is the quadratic bidirectional buck-boost converter, which facilitates energy flow between the motor, battery, and other energy sources while maintaining voltage stability across varying load conditions. In addition, using RES in EVs requires MPPT to make sure the PV system captures the maximum possible energy. MPPT algorithms always adjust the operating point of the PV panel to extract the highest possible power under changing irradiance levels [7]. However, traditional MPPT methods may suffer from slow convergence and inefficiencies under dynamic conditions, necessitating improvements in the control strategy.

ANNs are very useful for solving complex control problems because they can learn from data, adapt to changes, and handle nonlinear relationships between inputs and outputs. In the context of electric vehicles, ANNs can be employed to develop a control system that intelligently manages the power distribution between multiple energy sources and the vehicle's motor. ANNs are particularly useful in predicting the system's behaviour under different operating conditions, enabling the controller to make informed decisions that optimize performance. Model Predictive Control (MPC) is commonly used in industrial settings because it can predict future system behavior and optimize control actions over a set period [8]. In EV configurations, MPC can be used to set the motor speed, manage energy flow between the sources, and ensure efficient battery charging. When combined with ANN, the MPC system can adapt to the nonlinear and time-variable properties of the hybrid EV system, providing superior control over traditional methods.

The integration of multiple energy sources and advanced control systems in EVs is topic of extensive research in recent years. Many studies have said the optimization of energy management in EVs using hybrid configurations that include RES such as PV cells and fuel cells. The following literature review examines recent advancements in this field and highlights some limitations and drawbacks in each study. In [9], a hybrid energy system was developed for EVs, combining a hydrogen fuel cell by a battery for energy storage. The authors used an MPC strategy to raise energy allocation in the fuel cell and battery, which led to improved efficiency. However, the study relied solely on battery storage, limiting the system's flexibility to integrate additional renewable sources such as PV cells.

In [10], a hybrid system relating a fuel cell and battery was proposed for electric buses, with a focus on extending driving range and reducing emissions. The study used an adaptive control method to manage the power flow between the fuel cell and battery while driving in different conditions. While the study achieved significant improvements in fuel efficiency, it did not incorporate renewable sources like PV systems, which could further reduce dependency on the fuel cell during operation. In [11], a hybrid electric vehicle configuration was introduced that integrates PV cells with a fuel cell to improve energy management. The researchers used an MPPT algorithm to optimize power extraction by the PV system. However, the MPPT control strategy used in the study showed slow convergence under rapidly changing irradiance, leading to suboptimal power generation from the PV cells during dynamic conditions.

In [12] developed a hybrid EV system that combined a fuel cell, battery, and PV array, along with an MPC-based control system to manage energy flow between the sources. The system demonstrated high efficiency under various driving scenarios. Despite its promising results, the system's complexity was increased due to the multiple control loops required to manage the different energy sources, making implementation more challenging in real-world applications. In [13] proposed a multi-source EV system utilizing fuel cells, batteries, and supercapacitors for optimal energy management. The system employed a fuzzy logic control approach to manage the power distribution in the unique energy sources. One limitation of this study was the lack of predictive control strategies, which could have improved the system's adaptability to real-time changes in load conditions.

In [14] focused on a hybrid energy management system for EVs using fuel cells and PV systems. The study implemented an Incremental Conductance (INC) MPPT process to optimize the power obtained from the PV array. While the system achieved high energy efficiency, the INC MPPT algorithm showed instability under partially shaded conditions, leading to decreased overall system performance. In [15] explored the integration of fuel cells and batteries in EVs with an emphasis on energy management through a hierarchical control strategy.

The study achieved efficient power distribution in the fuel cell, battery but failed to consider the potential of incorporating renewable sources such as PV panels, which could further optimize energy use and reduce reliance on the grid.

In [16], a new control system for hybrid EVs was introduced, using fuzzy logic to manage energy in a fuel cell, battery, and supercapacitor. While the fuzzy logic controller provided flexibility in power management, it lacked the predictive capabilities that could enhance the system's performance, particularly under varying load and driving conditions. In [17] a hybrid fuel cell and battery system were proposed for electric vehicles, controlled by an adaptive MPC system. The adaptive MPC achieved high efficiency by optimizing energy flow between the two sources. However, the study did not account for PV integration, which could have improved the overall system's sustainability and reduced its reliance on non-renewable fuel cells.

In [18] presented an EV configuration integrating fuel cells and batteries, with an emphasis on improving driving range through optimal energy management. The system used a traditional Proportional-Integral-Derivative (PID) control strategy to regulate energy flow, but this approach lacked the adaptability of modern control strategies such as ANN-based MPC, which could have enhanced the system's dynamic response. While significant advancements have been made in the development of hybrid EV systems, many studies have focused on integrating fuel cells and batteries, with limited exploration of PV systems. Additionally, many control strategies employed, such as fuzzy logic and PID, lack the predictive capabilities of more advanced systems like ANN-based MPC [19]. The current research aims to address these gaps by integrating a fuel cell, electrolyzer, and PV system in a single EV configuration and employing an ANN-based MPC for optimized control and energy management.

For issues, this paper presents a new EV setup that combines a fuel cell, an electrolyzer, and an onboard PV cell, all managed by an advanced MPC system by ANN [20]. The motivation behind this study is to develop a novel EV configuration that optimizes the power management between different energy sources, improves the efficiency of energy conversion, and ensures smooth operation under varying environmental conditions [21]. The proposed system aims to minimize energy losses, enhance driving range, and reduce the overall cost of operation, making EVs more practical and appealing for widespread use.

The initial object of this study is to develop and analyse an advanced EV design that integrates a fuel cell, electrolyzer, and PV system with an ANN-based MPC control strategy [22]. The specific goals of this study include:

- 1. Designing an EV system that maximizes the use of RES, like PV cells and fuel cells, to improve energy efficiency and lower emissions.
- 2. Developing a quadratic bidirectional buck-boost converter for efficient energy management between the motor, battery, and energy sources.
- 3. Implementing an ANN-based MPC control system to set motor speed and improve power quality.
- 4. Incorporating an improved MPPT algorithm to reach energy extraction from the PV system.
- 5. Running simulations in MATLAB/SIMULINK to measure the performance of the future EV design under different levels of irradiance and speed.

This study aims to improve EV technology by combining RES with smart control systems be reliable, and sustainable transportation solution.

2. Proposed Electric Vehicle with Solar Onboard

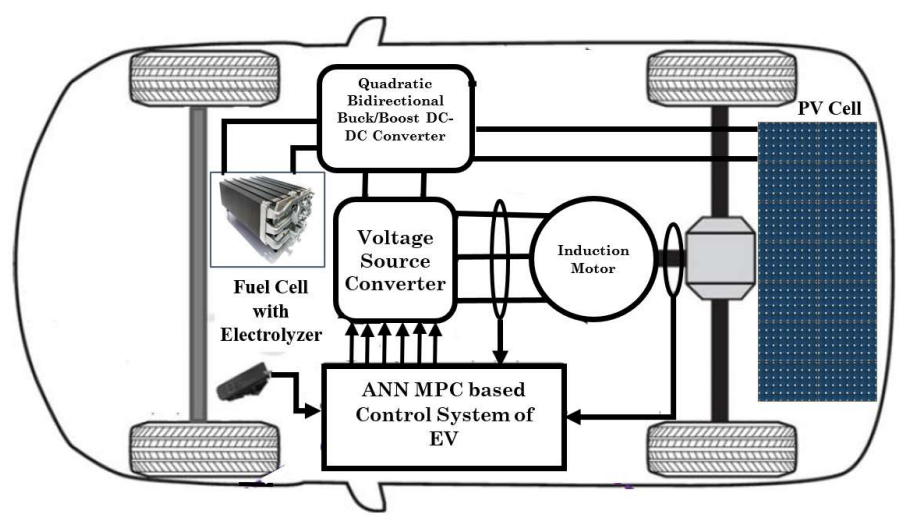


Fig 1. Outline of Hybrid Electric Vehicle

To ensure continuous power in a cost-effective and reliable manner, an energy storage system is essential, although it may affect reliability and availability. In the 21st century, solar energy and fuel cell technologies are seen as useful and eco-friendly ways to generate power. Each technology has its own strengths and weaknesses. Combining solar energy and fuel cells in Hybrid EVs can enhance both efficiency and reliability. Figure 1 shows a typical EV setup that includes solar and fuel cell components.

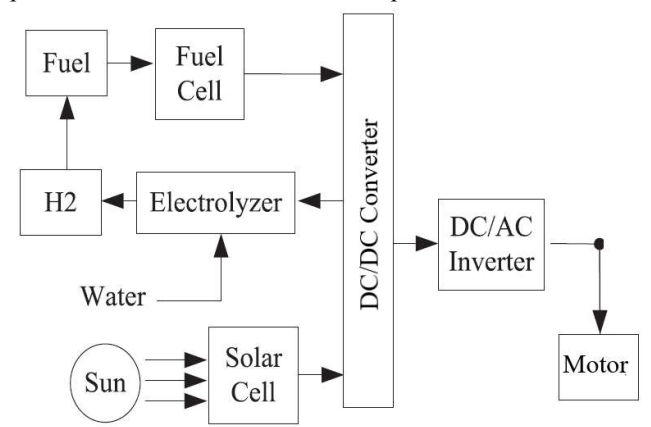


Fig 2. Configuration of PV and FC in proposed HEV

HEVs use DC-DC bidirectional boost-buck converters, allowing power to flow in directions. High-gain boost converters are a key area of research in power electronics because of their growing use in applications like fuel cell systems, distributed photovoltaic generation, and uninterruptible power supplies. In these applications, reaching a relatively high gain (V_{out}/V_{in}) is crucial. However, traditional boost converters aren't ideal for very high step-up gains because they face problems like very short switch-off times, high voltage stress on the switches, and low efficacy. So, there's a need for high-gain, efficient converters to overcome these problems. The voltage boost in a converter with coupled inductors can be enhanced by adjusting the duty cycle or increasing the turns ratio of the inductor. A common issue with these converters is the high input current ripple. Quadratic converters have attracted attention from power electronics researchers because they can boost the voltage more than traditional converters while solving some problems found in other methods.

One of the key components of the proposed EV configuration is the onboard PV cell, which harnesses solar energy to supplement the fuel cell and battery. So that the PV system operates at its maximum potential, a MPPT algorithm is employed. MPPT algorithms constantly adjust the PV panel's operating point to maximize energy extraction despite changes in solar irradiance and temperature.

This paper introduces an improved incremental conductance algorithm for MPPT, which enhances the efficiency of the PV system by achieving faster convergence and reducing energy losses. The improved algorithm is designed to operate effectively under dynamic conditions, ensuring that the PV system always runs at its optimal point. By incorporating this advanced MPPT control strategy, the proposed EV configuration maximizes the use of renewable energy, further reducing the vehicle's dependency on external energy sources.

3.1. Electrolyzer

The Unipolar Stuart cell is recognized for its high efficiency, low allowance and robust consistency. It operates with electrode having a single polarity, resulting in the making of $H_2(cathode)$ or $O_2(anode)$. The electrolyzer is made with several cells, each included in separate sections. Under normal conditions, the cell voltages typically range from 1.7 to 1.9 V. The electrolyte circulates as H_2 and O_2 gases rise done the channels in the electrodes and the cell separator. The electrolyzer works at temperatures below 70° C, reducing stress on materials. It produces hydrogen (H_2) with 99.9% purity and operates with 100% current efficiency, ensuing in a high hydrogen production rate.

$$X_{H_Z} = 5.18e^{-6}I_e mole/s \tag{1}$$

The current in the electrodes (I_e) enables the storage of hydrogen H_2 at 3 bars in a tank. This saved hydrogen is to supply power during periods of low sunlight and is later used to feed the fuel cell (FC).

3.2. Fuel cell

A notable point in the system design is the factor that impacts the electrolysis process, especially after sunset when the electrolyzer current drops to zero. To avoid undue corrosion of the cathodic potential, the electrolyzer must be maintained under a protective voltage during this period. To address this issue, the future electric storage device is planned to separate the electrolyte by the electrolysis cell. It introduces N_2 in the electrolyzer as a protective measure to prevent corrosion on the electrodes, as shown in Figure 1. In the intended system, air acts as the oxidant, and the cell operates at atmospheric pressure and 70°C. The current density is set at 400 mA/cm², which requires using 90 fuel cells stacked together. At atmospheric pressure, the Nernst equation combines the electrical operation of the fuel cell with its operating terms [4].

$$V_o = E_o + \frac{R.T}{2F} \ln \frac{x_{H_2} x_{O_2}^{0.5}}{x_{H_2O}}$$
 (2)

4. Quadratic Bidirectional Boost/Buck DC-DC Converter

Figure 1 shows the power setup of the Quadratic Bidirectional Boost/Buck DC-DC converter. Unlike the traditional Boost quadratic converter, this design doesn't need extra passive components like inductors or capacitors in the power circuit. It has a fixed voltage gain with a quadratic function for both Boost and Buck modes. The converter's charging and discharging are managed by a single transistor. To analyze its behavior, the bidirectional DC/DC converter will be examined in steady-state operation, operating in different modes: Boost mode and Buck mode. In the forward mode, the converter acts as a Boost converter, transferring energy from the input to the output. Two IGBTs (T1 and T4) are kept continuously OFF, while IGBT T3 remains continuously ON. By using PWM with a switching period of Tc , the output voltage and inner current for IGBT T2 can be controlled. When IGBT T2 is ON during the time interval Δ Ts, the inductors L1 and L2 charge with a steadily increasing current, shifting energy from the capacitor C to inductor L2. Conversely, during the time interval $1-\Delta$ Ts , when IGBT T2 is OFF, the inductors L1 and L2 discharge by a gradually decreasing current, sending energy to the capacitor and the output.

During Boost Mode

$$\Delta V_{in} + (1 - \Delta)(V_{in} - V_c) = 0$$

$$\Delta V_c + (1 - \Delta)(V_c - V_{out}) = 0$$
(3)

Then voltage gain is as

$$G = \frac{V_{out}}{V_{in}} = \frac{1}{(1 - \Delta)^2} \tag{5}$$

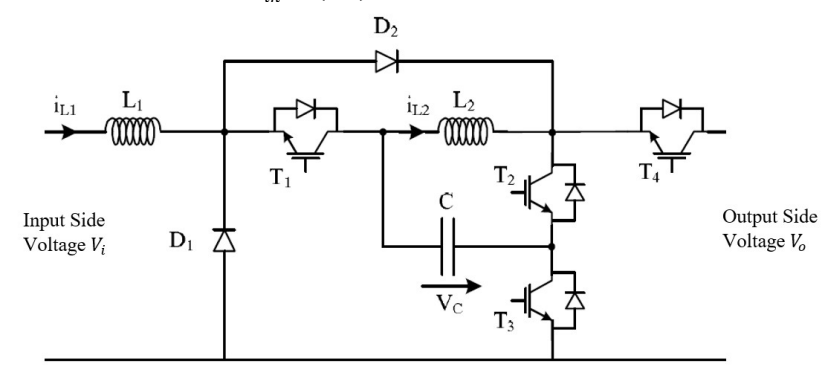


Fig 3. Schematic of QBBC

In this mode, the converter functions as a Buck converter, transferring energy from the output side to the input side. IGBTs T2 and T3 stay continuously OFF, while T4 stays continuously ON. By PWM with a switching period of Tc, T1 can be controlled through output voltage and inner current control. When T1 is ON in the time interval

 ΔTs , the currents in inductors L1 and L2 increase steadily as capacitor C discharges, sending its energy to inductor L1. Conversely, during the time interval $1-\Delta Ts$, when T1 is OFF, the currents in inductors L1 and L2 drop steadily. The energy stored in the inductors is transferred to capacitor C and then to the input side of the converter.

During Buck Mode

$$\Delta(V_c - V_{in}) - (1 - \Delta)V_{in} = 0$$

$$\Delta(V_c - V_{out}) + (1 - \Delta)V_c = 0$$
(6)

Then voltage gain is given as

$$G = \frac{v_{in}}{v_{out}} = \Delta^2 \tag{8}$$

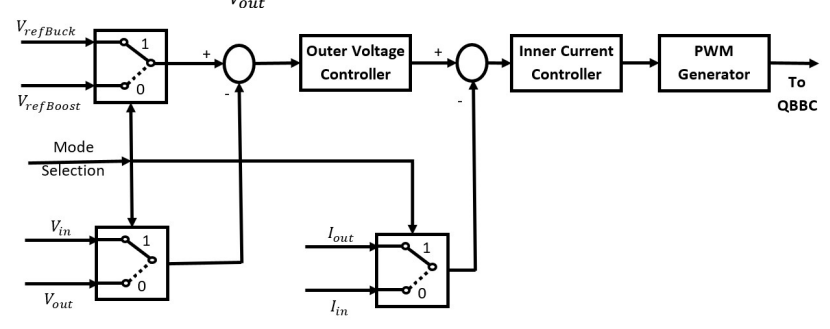


Fig 4. QBBC controlling

Figure 3 shows how the bidirectional DC-DC converter is controlled, supporting buck and boost modes. The converter switches between these modes based on the control of power flow or current. The DC-DC converter control uses two loops: an outer voltage control loop to manage the voltage and an inner current control loop to manage the current. Both loops are controlled using PI controllers. The benefits of the proposed converter are: (i) It has low input current ripple and conduction loss, making it suitable for low-to-medium power applications. (ii) The converter provides a much higher voltage boost than a traditional quadratic boost converter. (iii) It also reduces voltage stress on the main switch and diodes compared to a traditional quadratic boost converter with the same output voltage.

4.1. Induction motor modelling

The driving force of the proposed EV configuration is an implied vector-controlled induction motor. The induction motor is known for its robustness, consistency, and ability to run over a large range of speeds. However, to achieve precise control of the motor's speed and torque, a better control strategy is required.

The proposed system utilizes an ANN-based Model Predictive Control (MPC) approach for motor speed regulation. Unlike traditional methods, such as Proportional-Integral (PI) controllers, the ANN-based MPC system can predict future states of the motor and adjust control signals accordingly. This predictive control approach enables the motor to operate more efficiently, particularly under varying load and speed conditions.

Besides speed regulation, the proposed system introduces a method for predictive torque control of the induction motor, removing the need for weighting factors. This approach simplifies the control algorithm while improving the motor's performance in terms of torque response and overall efficiency. An ANN estimator is employed to predict motor speed and stator current in real time, further enhancing the precision and consistency of the control system.

The induction motor is ideal in EVs and HEVs due to its performance compared to other motor types. It can rapidly reach the desired speed while maintaining energy use in safe current limits, whether operating in generator or motor mode [15,25,26]. An induction motor (IM) can be modelled as a fifth-order system, including variables like speed, rotor flux, and stator currents. The stator and rotor currents are split into two parts: direct (d) and quadrature (q) axis components. Therefore, the fifth-order state variables of the IM can be stated as follows:

$$\frac{di_{sd}}{dt} = \frac{L_r R_s + \frac{M^2}{\tau_r}}{\rho L_r L_s} i_{sd} + \omega_g i_{sd} + \frac{M}{\rho \tau_r L_r L_s} \psi_{rd} + \frac{M}{\rho \tau_r L_r L_s} \psi_{rd} \omega_r + \frac{1}{\rho L_s} v_{sd}$$

$$\frac{di_{sq}}{dt} = \frac{L_r R_s + \frac{M^2}{\tau_r}}{\rho L_r L_s} i_{sq} - \omega_g i_{sd} + \frac{M}{\rho \tau_r L_r L_s} \psi_{rq} + \frac{M}{\rho L_r L_s} \psi_{rd} \omega_r + \frac{1}{\rho L_s} v_{sq}$$

$$\frac{d\psi_{rd}}{dt} = \frac{M^2}{\tau_r} i_{sd} - \frac{M}{\tau_r} \psi_{rd} + (\omega_g - \omega_r) \times \psi_{rq}$$

$$\frac{d\psi_{rq}}{dt} = \frac{M^2}{\tau_r} i_{sq} - \frac{M}{\tau_r} \psi_{rq} - (\omega_g - \omega_r) \times \psi_{rd}$$

$$\frac{d\omega_r}{dt} = \frac{3npM}{2JL_r} (i_{sq}\psi_{rd} - \psi_{rq}i_{sd}) - \frac{B}{J} \omega_r - \frac{1}{J} T_L$$

where τ_r is the rotor time constant, set by $\tau_r = \frac{L_r}{R_r}$, and ρ is the leakage constant, set by $(L_r \times L_s M^2)/(L_r \times L_s)$.

Other notations are as follows: v_{sd} and v_{sq} are the d-axis and q-axis of the stator voltage, are the d-axis and qaxis of the stator current, and ψ_{rd} , ψ_{rq} are the d-axis and q-axis of the rotor flux. where L_s and L_r are the stator and rotor inductances, R_s is the stator resistance, M is the mutual inductance in the stator and rotor, ω_q is the synchronous reference frame speed, ω_r is the rotor speed in electrical radians per second, J is the total inertia, B is the viscous friction coefficient, np is the sum of poles, and TL is the load torque. The electrical dynamics of the IM are meant by Equations (12) through (15), while Equation (16) describes the mechanical motion dynamics of the motor.

5. Indirect field-oriented control

IFOC is the best method for controlling IMs by regulating the stator currents. It converts the three-phase stator currents to two orthogonal components, known as d-q coordinates. The flux is controlled by the d-axis component of the current i_s , as the q-axis component i_{sd} controls the motor torque. Figure 3 shows the basic IFOC scheme [27,28]. In usual, the d-axis and q-axis current factors i_{sd} and i_{sq} are shared with their reference values. Two PI controllers then process the error signals to verify the reference values for the voltage components V_{sd} and V_{sa} . The Clarke transformation is to convert these reference voltages into the stationary reference frame.

The switching signals for the VSI are generated using SVPWM to control the basic voltage to the induction motor. The three-phase inverter is powered by a DC voltage from the battery.

6. Model Predictive Control

6.1. Inverter Model

This study uses a two-level voltage source inverter (2L-VSI), shown in Fig. 1. Although it creates a lot of harmonics, it is chosen for its naivety and effective power change. All output leg of the 2L-VSI has two power switches that act in opposite pairs. Figure 2 shows the eight possible voltage vectors made by the 2L-VSI. Among these vectors, v_0 and v_7 are the null voltage vectors, where $(v_{\alpha} = 0; v_{\beta} = 0)$. This work focuses mainly on the control strategy, which is why this simple inverter has been selected.

The equations that depict the 2L-VSI are as:

$$v_a = S_a \frac{V_{dc}}{2}$$

$$v_b = S_b \frac{V_{dc}}{2}$$

$$v_c = S_c \frac{V_{dc}}{2}$$

The voltage in $\alpha - \beta$ frame can be as

$$\begin{bmatrix} v_{\alpha} \\ v_{\beta} \end{bmatrix} = \frac{2}{3} V_{dc} \begin{bmatrix} 1 & -0.5 & -0.5 \\ 0 & \sqrt{3}/2 & -\sqrt{3}/2 \end{bmatrix} \begin{bmatrix} S_{a} \\ S_{b} \\ S_{c} \end{bmatrix}$$

6.2. Motor Model

The mathematical model of the IM by the stator flux Ψs and stator current i_s as state variables. In a stationary the dynamic equations frame, were as

$$v_s = r_s i_s + \frac{d\lambda_s}{dt}$$

$$0 = r_s i_r + \frac{d\lambda_r}{dt} - j \frac{\omega_r}{p} \lambda_r$$

$$\lambda_s = L_s i_s + L_m i_r$$

$$\lambda_r = L_m i_s + L_r i_r$$

$$T = \frac{3}{2} p |\lambda_s \otimes i_s|$$

$$J \frac{d\omega_r}{dt} = T_e - T_L$$

To assume the torque and flux, it is key to quote the stator flux (λ_s) and the rotor flux (λ_r) at the current sampling time (k). The rotor flux can be estimated by the rotor dynamics equation of the induction motor (IM) in a rotating source frame seen by the rotor winding, are given as:

$$\psi_r + \tau_r \frac{d\psi_r}{dt} = L_m i_s$$

 $\psi_r + \tau_r \frac{d\psi_r}{dt} = L_m i_s$ The rotor time constant ($\tau_r = L_r/R_r$) is important. Using the backward-Euler method by a sampling time (T_s), the equation to estimate the rotor flux in discrete time is as.

$$\lambda_r^k = L_m \frac{T_s}{T_r} i_s^{k-1} + \left(1 - \frac{T_s}{T_r}\right) \lambda_r^{k-1}$$

The stator flux can be assessed by

$$\lambda_s^k = \frac{L_m}{L_r} \lambda_r^k + \left(1 - \frac{L_m^2}{L_s L_r}\right) i_s^k$$

Now, the stator flux estimate is got by the forward-Euler discretization:

$$\lambda_s^{k+1} = \lambda_s^k + T_s v_s^k - T_s R_s i_s^k$$

Now, the stator flux estimate is got by the forward-Euler discretization. $\lambda_s^{k+1} = \lambda_s^k + T_s v_s^k - T_s R_s i_s^k$ The stator current prediction is made by the forward-Euler discretization: $i_s^{k+1} = C_1 i_s^k + C_2 \lambda_s^k + \frac{T_s}{L_\sigma} v_s^k$

$$i_s^{k+1} = C_1 i_s^k + C_2 \lambda_s^k + \frac{T_s}{L_s} v_s^k$$

where $R_{\sigma} = (R_s + (L_m/L_r)^2 R_r)$ relates to the equivalent resistance, $C_1 = (1 - (R_{\sigma}T_s/L_{\sigma}))$, $L_{\sigma} = \sigma L_s$ is the leakage inductance of the machine and $C_2 = (L_m/L_r)T_s/L_{\sigma}((1/\tau_r) - j\omega^k)$ Finally, the torque prediction relies on the estimated stator flux and stator current and written as follows:

$$T^{k+1} = \frac{3}{2}p\big|\lambda_s^{k+1} \otimes i_s^{k+1}\big|$$

7. Online Artificial Neural Network Speed Estimator

This study employs an ANN-MPC system to manage the motor's speed and regulate the energy flow in the fuel cell, PV cell, and electrolyzer. The proposed system predicts future system states, calculates the optimal control actions, and updates the control plan based on real-time feedback. The ANN-MPC system offers several advantages, including improved energy efficiency, better power quality, and enhanced driving performance. From mathematical model of induction motor

$$\begin{bmatrix} v_{ds} \\ v_{qs} \\ 0 \\ 0 \end{bmatrix} = \begin{bmatrix} r_s + L_s \frac{d}{dt} & 0 & L_m \frac{d}{dt} & 0 \\ 0 & r_s + L_s \frac{d}{dt} & 0 & L_m \frac{d}{dt} \\ L_s \frac{d}{dt} & \omega_r L_m & r_r + L_r \frac{d}{dt} & \omega_r L_r \\ -\omega_r L_m & L_m \frac{d}{dt} & -\omega_r L_r & r_r + L_r \frac{d}{dt} \end{bmatrix} \begin{bmatrix} i_{ds} \\ i_{qs} \\ i_{dr} \\ i_{qr} \end{bmatrix}$$

Stator current can be said as

$$\frac{d}{dt} \begin{bmatrix} \hat{\iota}_{ds} \\ \hat{\iota}_{qs} \end{bmatrix} = \begin{bmatrix} -\frac{r_s^*}{L_{\sigma}} & -\omega_r & \frac{r_r}{L_{\sigma}L_r} & \frac{\omega_r}{L_{\sigma}} \\ \omega & -\frac{r_s^*}{L_{\sigma}} & \frac{\omega_r}{L_{\sigma}} & \frac{r_r}{L_{\sigma}L_r} \end{bmatrix} \begin{bmatrix} \hat{\iota}_{ds} \\ \hat{\iota}_{qs} \\ \hat{\lambda}_{ds} \\ \hat{\lambda}_{qs} \end{bmatrix} + \frac{1}{L_{\sigma}} \begin{bmatrix} v_{ds} \\ v_{qs} \end{bmatrix}$$

By the forward rectangular rule and differing the equation for ANN function, the discrete-time estimate of the stator current is given by:

$$\begin{bmatrix} \hat{l}_{sd}^k \\ \hat{l}_{sq}^k \end{bmatrix} = \left(1 - \frac{T_s r_s^*}{L_\sigma}\right) \begin{bmatrix} \hat{l}_{sd}^{k-1} \\ \hat{l}_{sd}^{k-1} \end{bmatrix} + \frac{T_s \omega_r}{L_\sigma} \begin{bmatrix} \hat{x}_{sd}^{k-1} \\ \hat{x}_{sq}^{k-1} \end{bmatrix} + \frac{T_s r_r}{L_\sigma L_r} \begin{bmatrix} \hat{\lambda}_{sd}^{k-1} \\ \hat{\lambda}_{sq}^{k-1} \end{bmatrix} + \frac{T_s}{L_\sigma} \begin{bmatrix} v_{ds}^{k-1} \\ v_{qs}^{k-1} \end{bmatrix}$$

This equation can be as

$$\vec{l}_{s}^{k} = w_{1}\vec{x}_{1} + w_{2}\vec{x}_{2} + w_{3}\vec{x}_{3} + w_{4}\vec{x}_{4}$$
Where $w_{1} = \left(1 - \frac{T_{s}r_{s}^{*}}{L_{\sigma}}\right)$, $\vec{x}_{1} = \begin{bmatrix} \hat{l}_{sd}^{k-1} \\ \hat{l}_{sd}^{k-1} \end{bmatrix}$, $w_{2} = \frac{T_{s}\omega_{r}}{L_{\sigma}}$, $\vec{x}_{2} = \begin{bmatrix} \hat{x}_{sd}^{k-1} \\ \hat{x}_{sd}^{k-1} \end{bmatrix}$, $w_{3} = \frac{T_{s}r_{r}}{L_{\sigma}L_{r}}$, $\vec{x}_{3} = \begin{bmatrix} \hat{l}_{sd}^{k-1} \\ \hat{l}_{sd}^{k-1} \end{bmatrix}$, $w_{4} = \frac{T_{s}}{L_{\sigma}}$ and $\vec{x}_{4} = \begin{bmatrix} v_{ds}^{k-1} \\ v_{ds}^{k-1} \end{bmatrix}$

Based on Equation (14), the ANN has two layers: the input and the output layer. The Widrow-Hoff learning rule is better for this type of ANN because it poses a basic weight update equation, better for online speed estimation than other methods.

So, the weight w₂ in Equation (14), which affects the speed, will be updated online by the Widrow–Hoff learning rule. This update aims to decrease the difference in the measured stator current and the estimated stator current. The error at sampling time k is stated by the energy function:

$$E = \frac{1}{2}((i_{sd}^k - \hat{i}_{sd}^k)^2 + (i_{sq}^k - \hat{i}_{sq}^k)^2)$$

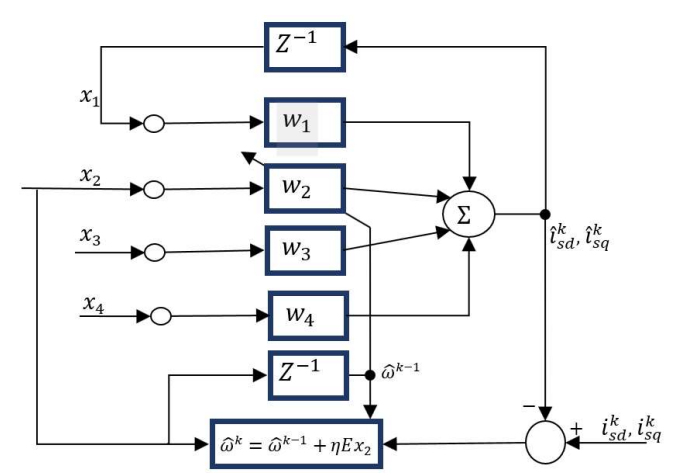


Fig. speed estimation by ANN

In Equation (18), only the weight w_2 is updated online. As a result, the precision of the valued stator current in matching the measured stator current varies on how well the expected speed converges. The speed estimate depicted by Equation (18) functions as a low-pass filter, with its time constant inversely shared to the learning rate. To keep stability, a positive learning rate is used. A small learning rate results in slow convergence, while a large learning rate speeds up convergence but affects variations in the estimated speed. So, opting for the right learning rate is key for keeping the estimation system stable.

8. Simulink model of proposed system

In this MATLAB/SIMULINK model of a hybrid electric vehicle (HEV), the primary objective is to assess the effectiveness of an advanced ANN-based Model Predictive Control (MPC) system for controlling the motor's speed. The configuration utilizes a fuel cell as the main power source, with a rooftop solar cell as a secondary source. Additionally, regenerative braking allows the system to store excess energy in a hydrogen tank by converting electrical energy into chemical energy through an electrolyzer. This comprehensive setup simulates the energy flow between multiple components, including the fuel cell, photovoltaic (PV) array, electrolyzer, and motor, all of which interact under different operating conditions.

Case 1:

In Case 1, the simulation focuses on a scenario where the reference speed of the motor is increased from 100 rad/s to 120 rad/s at the 10-second mark, while the irradiation remains constant at 1000 W/m². As illustrated in fig 8a, the PV array generates power at this fixed irradiation level, reaching approximately 2.01 KW. The output voltage from the PV system is boosted to 400V using a DC-DC boost converter, which operates under the Maximum Power Point Tracking (MPPT) method, specifically using the Incremental Conductance algorithm. This algorithm ensures that the PV system operates at its peak efficiency by adjusting the voltage and current in response to environmental changes. The result, as shown in fig 8b, is a stable boost of voltage, current, and power output from the PV converter, ensuring consistent energy delivery to the vehicle's electrical system.

Simultaneously, the fuel cell generates electricity to serve as the main power source, with its voltage, current, and power depicted in fig 9a. The fuel cell output is further regulated using a converter, whose voltage, current, and power characteristics are illustrated in fig 9b. The fuel cell operates in conjunction with the PV array to ensure a continuous supply of power, supporting the vehicle drive, particularly when the motor speed increases during the second half of the simulation. The electrolyzer, which operates during regenerative braking, also shows consistent voltage, current, and power characteristics, as demonstrated in fig 10.

A key component of the simulation is the Quadratic Bidirectional Buck-Boost Converter (QBBC), which elevates the input voltage from 400V (PV and fuel cell) to 780V to meet the operational requirements of the vehicle's drive system. Fig 11a displays the converter's input and output voltages, showing how effectively it handles the voltage boost necessary for motor control. The QBBC's performance is crucial for maintaining efficient power flow to the motor, ensuring the system's stability during acceleration and deceleration phases.

The core of the study focuses on the motor's speed control, where the performance of the traditional PI controller is compared to that of the proposed ANN-based MPC. Initially, the motor operates under vector control, with the reference speed held at 100 rad/s until the 10-second mark, after which it is increased to 120 rad/s. Fig 11b shows the three-phase stator currents controlled by the PI controller, while fig 13 highlights the stator current under ANN MPC control. The use of ANN MPC significantly reduces Total Harmonic Distortion (THD) in the stator current, decreasing it from 5.3% with the PI control to 2.8%, indicating smoother motor operation and reduced electrical noise.

The results further demonstrate how ANN MPC outperforms PI control in terms of speed and torque regulation,

as shown in fig 12. Under ANN MPC, the motor exhibits reduced peak overshoot, faster rise time, and a shorter settling time compared to PI control. These improvements in motor dynamics lead to more stable vehicle operation, especially during transitions in speed, highlighting the ANN MPC's superior ability to predict and adjust motor parameters in real time. The ANN-based MPC system demonstrates notable advantages over traditional PI control, particularly in terms of enhanced motor control, reduced harmonic distortion, and better overall system stability. The integration of renewable energy sources, combined with advanced control strategies, provides an efficient and reliable power solution for hybrid electric vehicles.

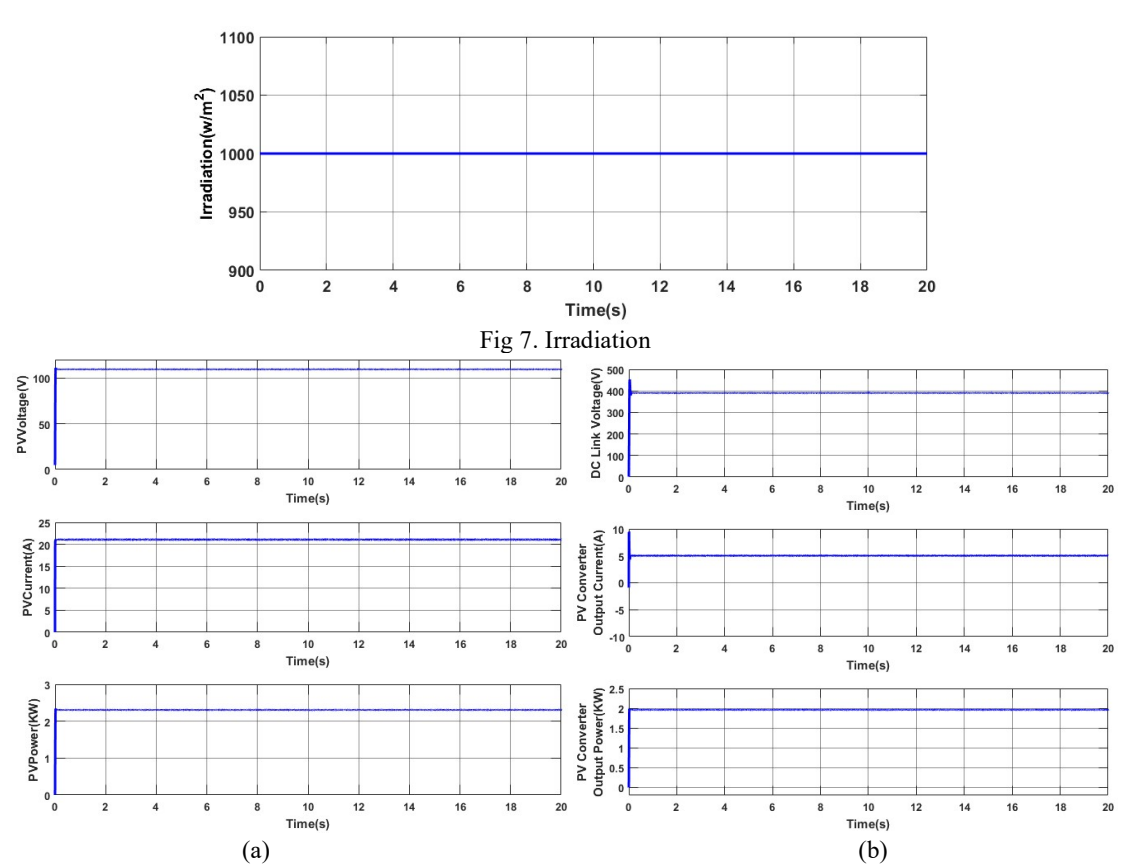


Fig 8. PV generation system (a) voltage in V, current in A and power in kW at PV terminals (b) voltage in V, current in A and power in kW at output terminal of PV DC/DC converter

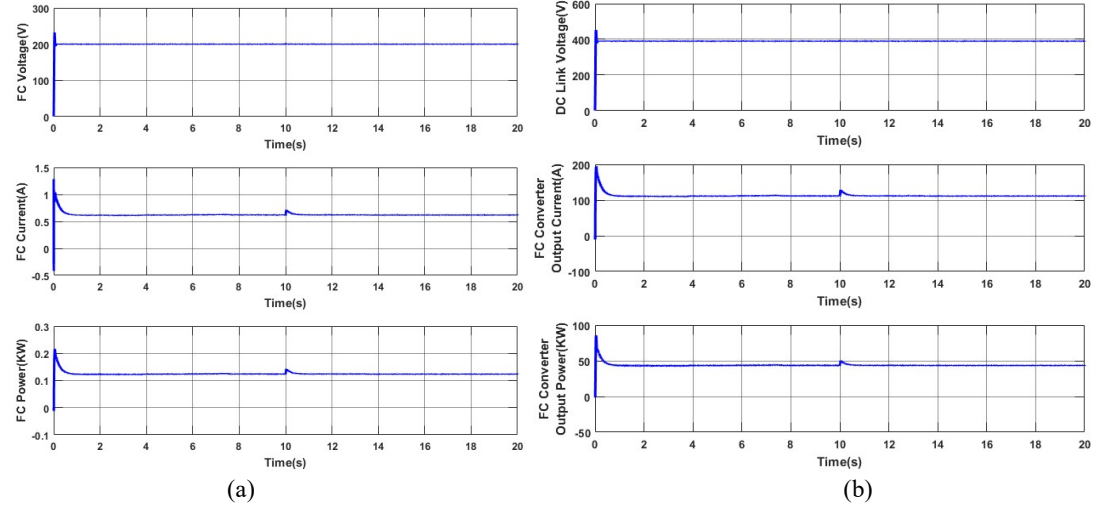


Fig 9. Fuel Cell system (a) voltage in V, current in A and power in kW at FC terminals (b) voltage in V, current in A and power in kW at output terminal of FC DC/DC converter

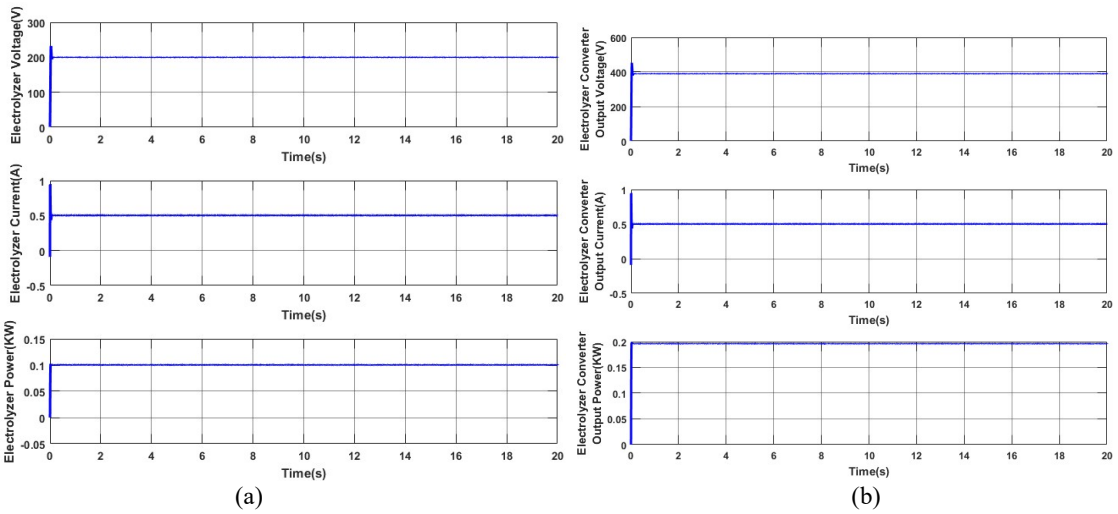


Fig 10. Electrolyzer system (a) voltage in V, current in A and power in kW at Electrolyzer terminals (b) voltage in V, current in A and power in kW at output terminal of Electrolyzer DC/DC converter

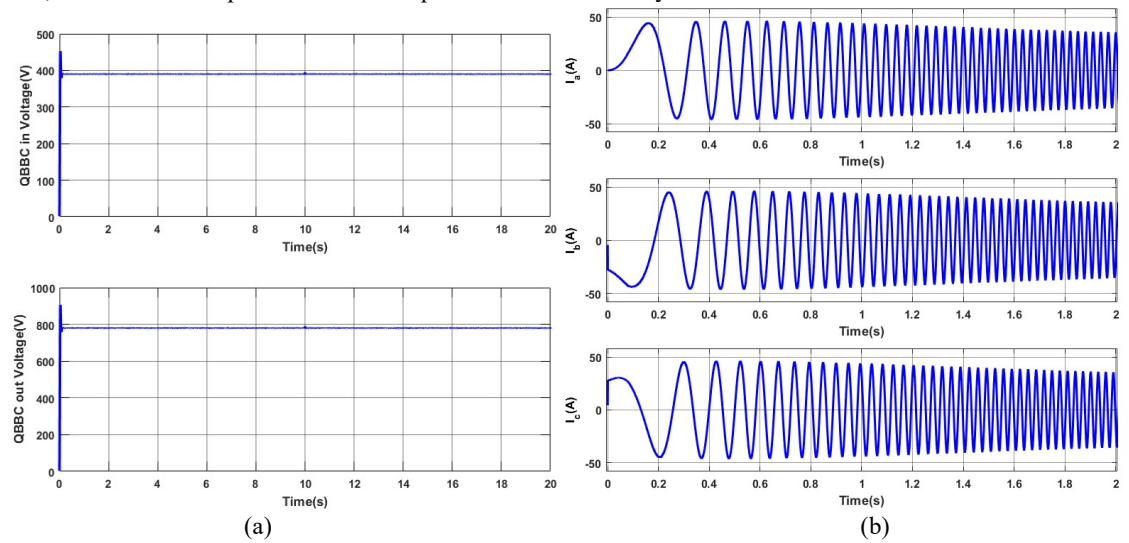


Fig 11. (a) Voltage in V at input output terminals of QBBC (b) stator currents in A during initial stage of motor running with convetional control

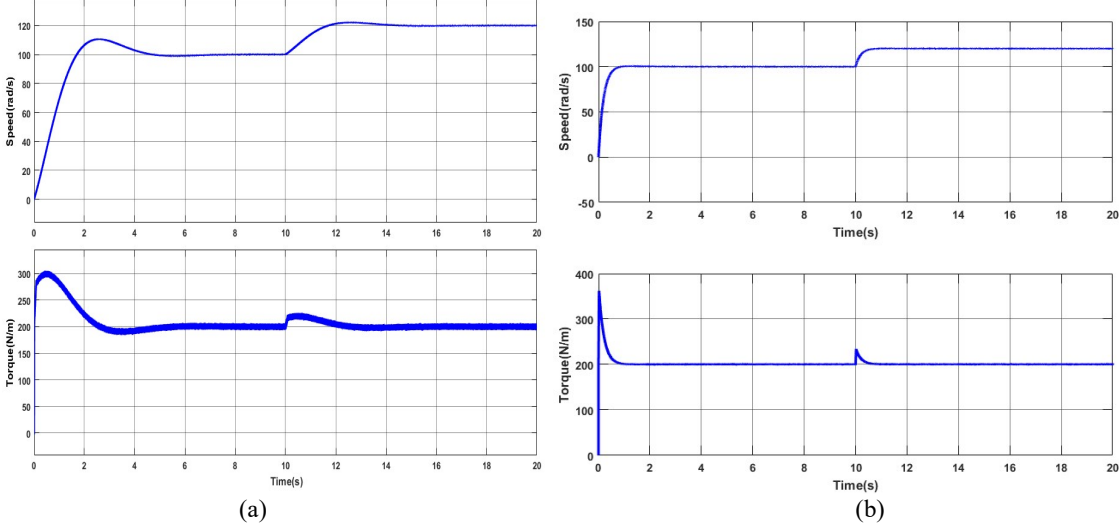


Fig 12. Speed in RPM and Torque in N/m (a) with PI Control (b) with Proposed Control

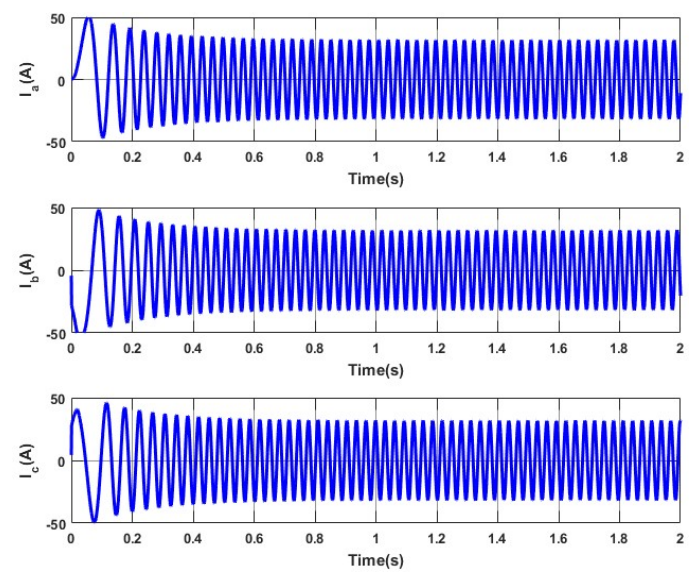


Fig 13. stator currents in A during initial stage of motor running with proposed control

Case2:

In Case 2, the proposed electric vehicle (EV) setup is tested under varying sunlight conditions, simulating real-world environmental changes. The motor's reference speed increases from 100 rad/s to 120 rad/s at 10 seconds, while the irradiance fluctuates between 600 W/m² and 1000 W/m², reflecting a dynamic solar power input. This scenario is designed to evaluate the system's ability to adapt to rapid changes in sunlight while maintaining stable motor operation and power generation from the fuel cell and solar PV array.

The PV array plays a critical role in this test, as it provides supplementary power to the fuel cell. The irradiance starts at 600 W/m² and gradually increases to 1000 W/m² before fluctuating back to 400 W/m² and then 900 W/m². As depicted in Figure 14, these changes directly influence the power generated by the PV array. Figure 15 displays the output voltage, current, and power of the PV system as it reacts to these irradiance changes. As the sunlight increases, the PV array produces more power, which is boosted by the MPPT-controlled DC-DC converter. Despite the fluctuating irradiance, the converter ensures that the output voltage is stabilized, providing consistent energy to the vehicle drive system.

One of the critical aspects of the system is the Quadratic Bidirectional Buck-Boost Converter (QBBC), which ensures that variations in irradiance do not impact the power supplied to the vehicle's drive inverter. As shown in Figure 18(a), the QBBC converter takes the fluctuating input voltage from the PV system and consistently boosts it to the required output voltage. Even as the irradiance changes, the converter's advanced control ensures that the voltage supplied to the vehicle drive remains unaffected, maintaining a steady output of 780V necessary for the motor's operation. This stable voltage regulation under variable irradiance is crucial for the EV's performance, allowing the system to function smoothly even with inconsistent solar power.

In addition to the PV system, the fuel cell operates as the primary power source, ensuring that the vehicle has sufficient energy, especially when solar power is low. Figure 16 shows the fuel cell's output voltage, current, and power as it interacts with its converter. The fuel cell provides a steady supply of energy, regardless of the changing irradiance, compensating for any drop in power from the PV system. The fuel cell converter regulates the output to meet the vehicle's power demands, ensuring that the system remains functional even when solar power generation is limited, such as during the 400 W/m² irradiance period. During this test, regenerative braking plays an essential role in energy storage. The excess energy generated by the PV system and the fuel cell is converted into chemical energy through the electrolyzer and stored in a hydrogen tank. Figure 17 illustrates the electrolyzer's voltage, current, and power as it operates in tandem with the rest of the system. The electrolyzer ensures efficient energy storage, which can later be used when the vehicle demands additional power or during braking phases. Its converter helps in regulating the energy flow, allowing for efficient conversion of electrical energy into hydrogen for storage.

The core objective of the simulation is to assess motor speed and torque control under varying irradiance conditions. As the reference speed increases from 100 rad/s to 120 rad/s at 10 seconds, Figure 19 compares the performance of the motor under traditional PI control versus the proposed ANN-based Model Predictive Control (MPC). The results show a clear advantage of ANN MPC in terms of speed and torque regulation. With ANN MPC, the motor achieves faster response times, reduced overshoot, and improved stability, especially under changing environmental conditions. The fluctuating irradiance does not affect the motor's ability to maintain the desired speed and torque with the ANN MPC system, thanks to its predictive capabilities, which allow it to adapt quickly to the variations in input power. In contrast, the PI controller exhibits slower response times and larger

overshoot, making the motor less efficient under rapidly changing power conditions. This is especially evident during the periods of lower irradiance, where the PI controller struggles to maintain stability. The ANN MPC, on the other hand, shows superior performance, providing smoother control with minimal fluctuations in speed and torque.

Overall, the simulation results from Case 2 demonstrate the robustness of the proposed EV system under varying sunlight conditions. The combination of the PV array, fuel cell, electrolyzer, and QBBC converter ensures a reliable and stable power supply, even when the irradiance fluctuates. The advanced control strategy provided by the ANN MPC significantly enhances motor performance, offering better speed and torque regulation compared to the traditional PI controller. This makes the proposed system highly effective for real-world applications, where environmental conditions can change rapidly, and reliable control is essential for maintaining optimal vehicle operation.

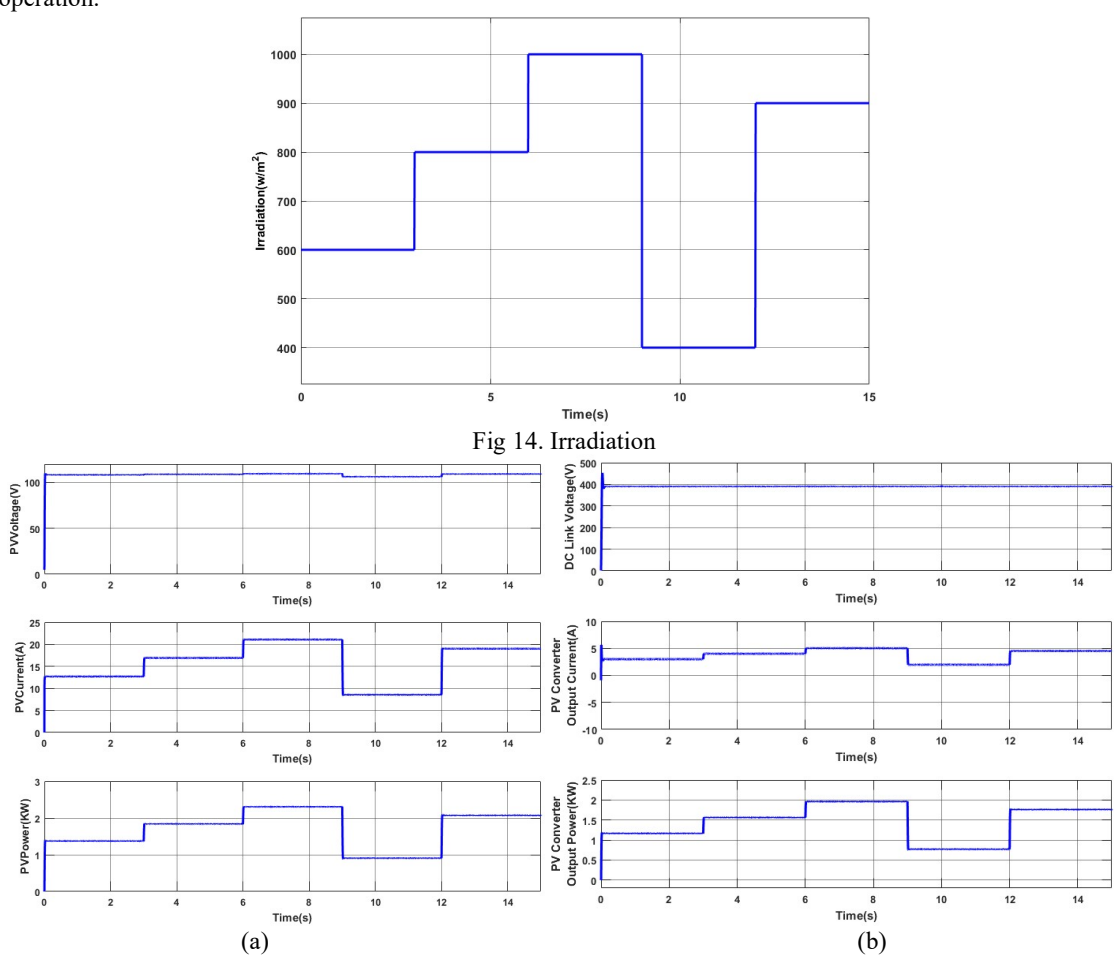


Fig 15. PV generation system (a) voltage in V, current in A and power in kW at PV terminals (b) voltage in V, current in A and power in kW at output terminal of PV DC/DC converter

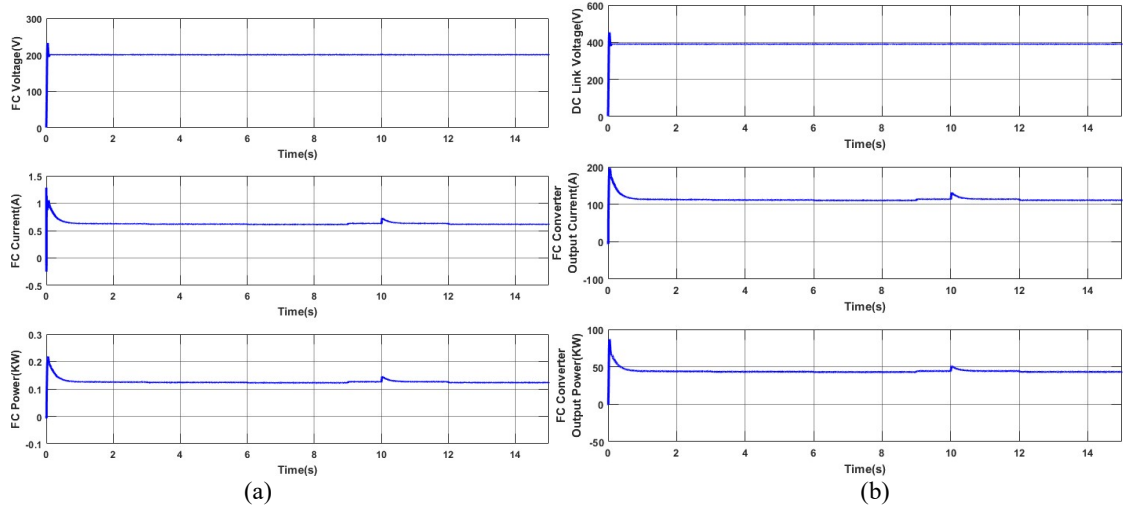


Fig 16. Fuel Cell system (a) voltage in V, current in A and power in kW at FC terminals (b) voltage in V, current in A and power in kW at output terminal of FC DC/DC converter

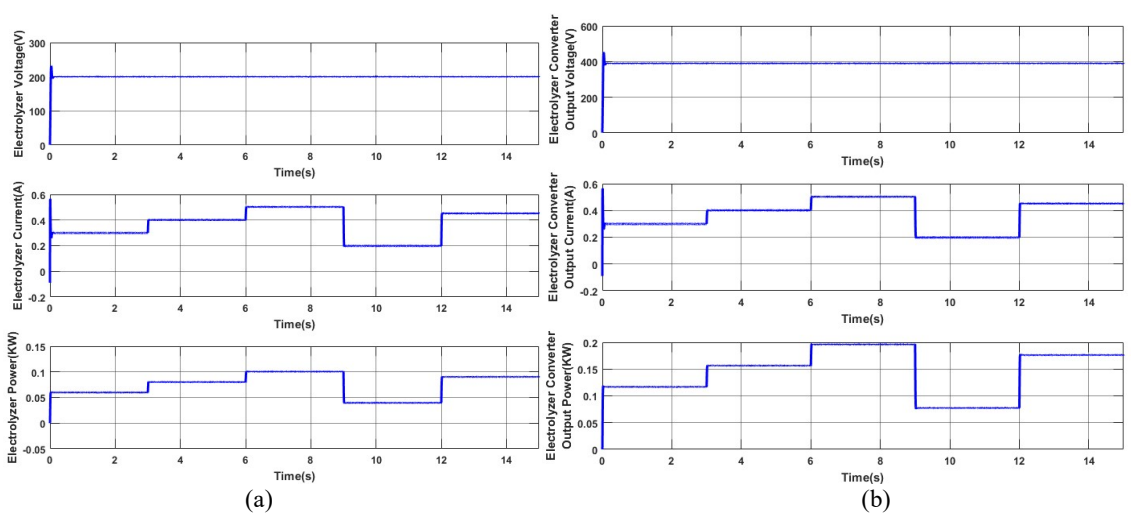


Fig 17. Electrolyzer system (a) voltage in V, current in A and power in kW at Electrolyzer terminals (b) voltage in V, current in A and power in kW at output terminal of Electrolyzer DC/DC converter

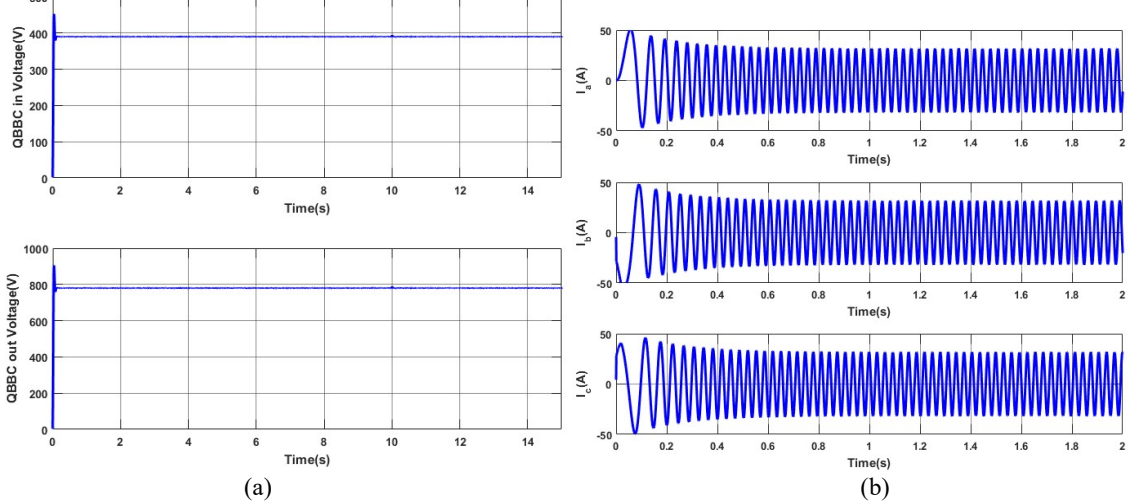


Fig 18. (a) Voltage in V at input output terminals of QBBC (b) stator currents in A during initial stage of motor running with convetional control

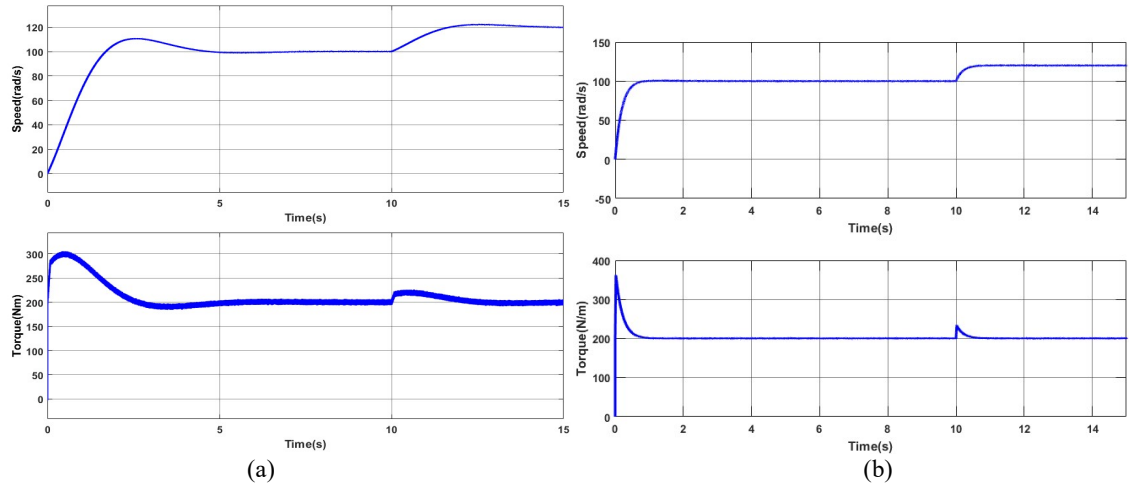


Fig 19. Speed in RPM and Torque in N/m (a) with PI Control (b) with Proposed Control

Case3:

In Case 3, the vehicle drive is tested under a constant irradiance of 1000 W/m² to evaluate how the system responds to a wide range of changes in motor speed. The speed increases and decreases over a 17.5-second interval, simulating realistic acceleration and deceleration scenarios. The performance of the Quadratic Bidirectional Buck-Boost Converter (QBBC), motor control system, and power sources (solar PV and fuel cell) are analyzed in this case, with a focus on comparing the traditional PI controller with the proposed ANN-based Model Predictive Control (MPC) method.

As the motor speed varies from 30 rad/s to 150 rad/s, the QBBC converter ensures a constant output voltage of 780V for the vehicle drive inverter. Figure 20(a) displays the input and output voltages of the QBBC converter. Despite the fluctuations in the motor's speed, the converter effectively stabilizes the voltage. The input voltage from the PV system or fuel cell fluctuates depending on the motor's power demands, but the output voltage remains consistent at 780V, ensuring smooth and reliable power delivery to the motor. This stability is critical for ensuring that the vehicle drive operates efficiently, particularly during rapid acceleration and deceleration periods. The core of the simulation is the motor speed and torque control under both the traditional PI controller and the proposed ANN-based MPC. The motor speed increases in stages—first from 30 rad/s to 50 rad/s at 2.5 seconds, then to 100 rad/s at 5 seconds, followed by 120 rad/s at 7.5 seconds, and finally 150 rad/s at 10 seconds. After reaching the peak of 150 rad/s, the speed is reduced in stages, first to 100 rad/s at 12.5 seconds, then 70 rad/s at 15 seconds, and finally down to 50 rad/s at 17.5 seconds.

Figure 21 illustrates how the motor speed and torque behave during these changes. Under the PI control, there is noticeable overshoot and slower response times during acceleration. The motor speed takes longer to stabilize after each change in the reference speed, and the torque shows significant fluctuations. In contrast, the ANN MPC exhibits much smoother transitions in both speed and torque. The predictive capabilities of ANN MPC allow it to adjust more effectively to changes in reference speed, resulting in faster response times, minimal overshoot, and a more stable torque output. The ANN MPC provides a significant improvement in motor control, especially during the rapid increases and decreases in speed, demonstrating its ability to maintain optimal performance in dynamic conditions.

Given the constant irradiance of $1000~W/m^2$, the PV system generates consistent power throughout the simulation. Figure 22(a) shows the output voltage, current, and power of the PV system, which remain relatively steady as the irradiance is fixed. However, the motor's varying speed demands different levels of power, which are supplemented by the fuel cell when the PV system alone cannot meet the vehicle's energy requirements.

Figure 22(b) displays the output voltage, current, and power of the fuel cell. The fuel cell acts as the primary energy source when the motor speed increases significantly, such as during the acceleration phases. It provides the additional power required by the motor while maintaining a stable output, ensuring that the vehicle has sufficient energy for its operation. The fuel cell's converter regulates this output, helping balance the energy supply between the PV array and the fuel cell.

Finally, Figure 24 illustrates the motor's active and reactive power. As the motor speed changes, the active power (responsible for performing mechanical work) fluctuates accordingly. During the acceleration phases, the active power increases significantly, reaching a peak at 150 rad/s, as the motor demands more power to achieve the higher speed. During deceleration, the active power decreases as less energy is required to maintain or reduce the speed.

The reactive power, which is essential for maintaining the magnetic fields within the motor, also fluctuates during these changes in speed. The ANN MPC system, however, shows better regulation of both active and reactive

power compared to the PI controller. The active power remains more stable with fewer spikes, and the reactive power is better managed, leading to more efficient motor operation, especially during the transition between different speed levels. This smooth management of active and reactive power helps reduce energy losses and improves the overall efficiency of the motor control system.

The simulation results from Case 3 demonstrate that the ANN-based MPC significantly outperforms the traditional PI controller in terms of motor speed and torque regulation, especially under varying speed conditions. The QBBC converter effectively stabilizes the output voltage, ensuring that the motor receives consistent power despite the changing speed. The PV system and fuel cell work together to provide a reliable energy supply, with the fuel cell compensating for the increased power demands during acceleration. The ANN MPC also ensures smoother transitions in active and reactive power, resulting in better motor performance, reduced energy losses, and overall improved system efficiency. This makes the proposed configuration highly suitable for dynamic driving conditions in electric vehicles.

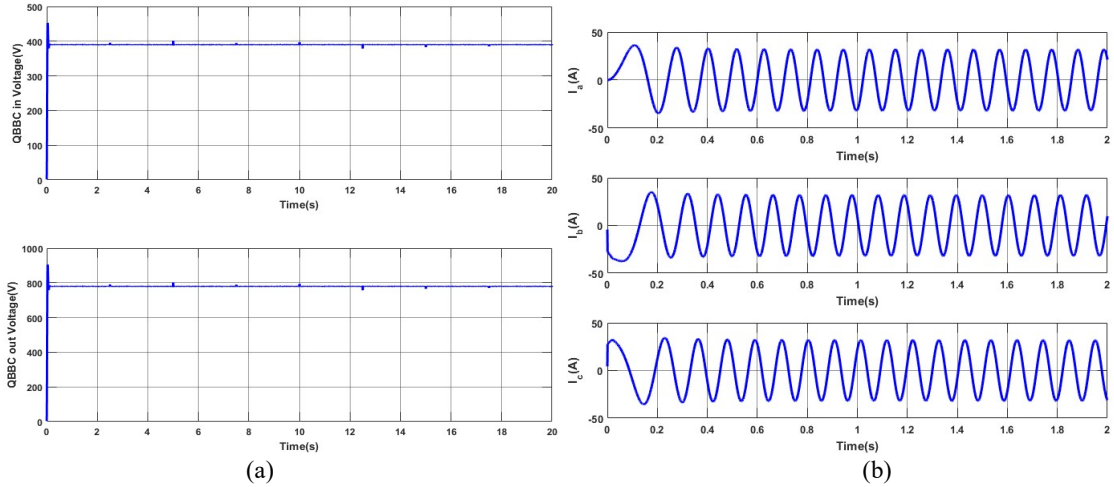


Fig 20. (a) Voltage in V at input output terminals of QBBC (b) stator currents in A during initial stage of motor running with proposed control

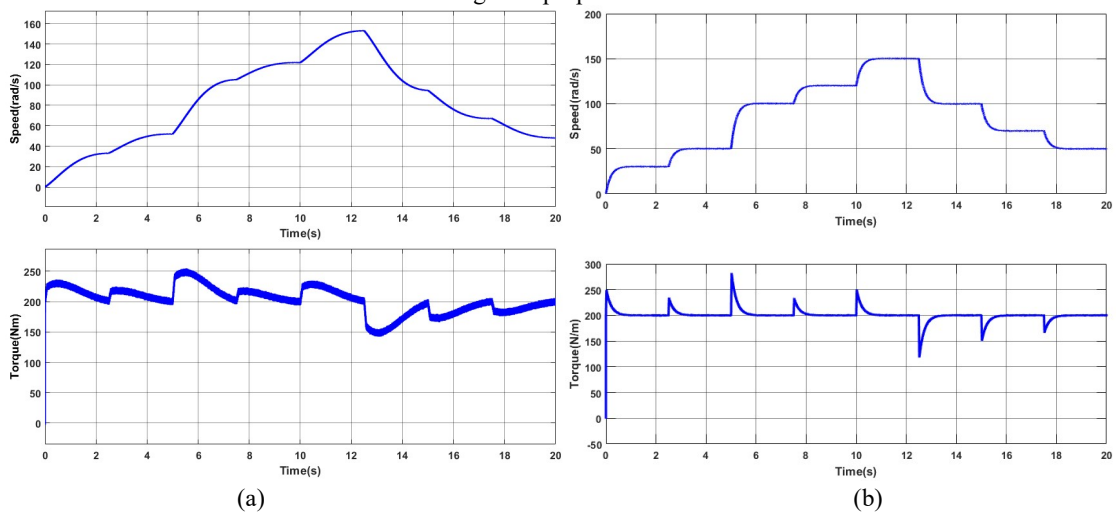


Fig 21. Speed in RPM and Torque in N/m (a) with PI Control (b) with Proposed Control

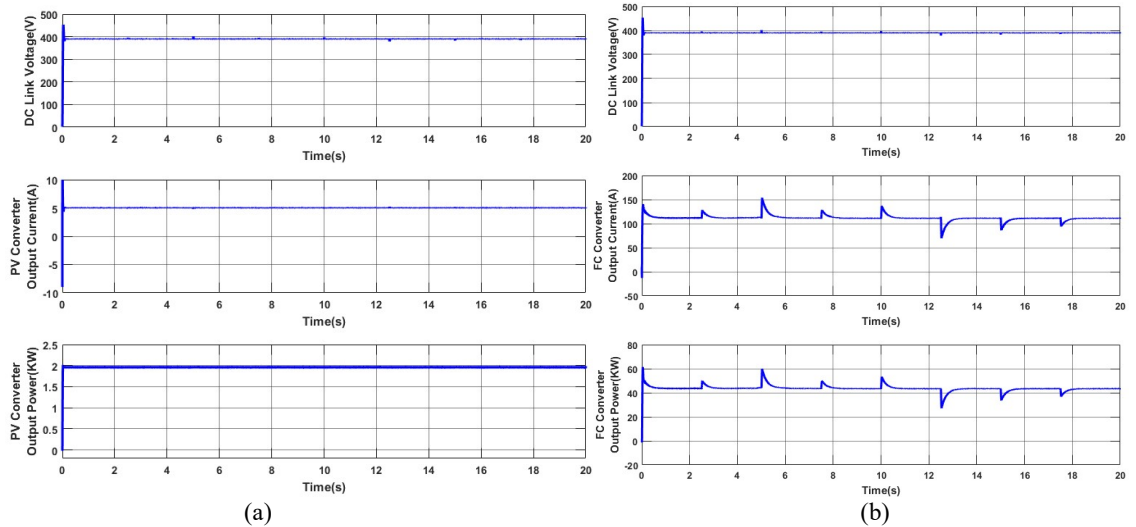


Fig 22. (a) voltage in V, current in A and power in kW at output terminal of PV DC/DC converter (b) voltage in V, current in A and power in kW at output terminal of FC DC/DC converter

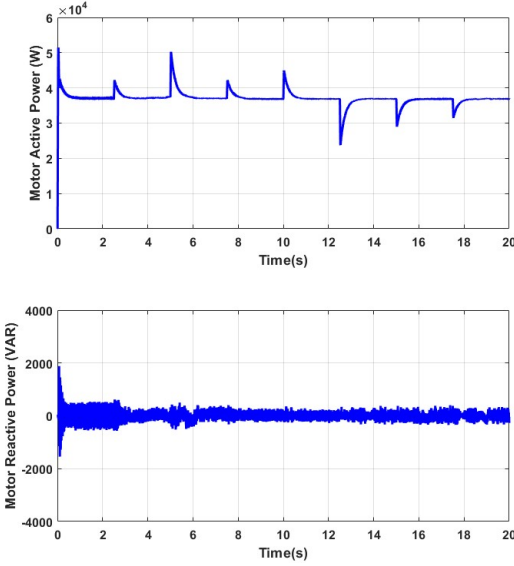


Fig 24. Motor Input active and reactive power with proposed control

Case4:

In Case 4, the electric vehicle (EV) system is tested under dynamic conditions where the motor speed and load torque change significantly over a 17.5-second period. The motor's reference speed increases rapidly from 100 rad/s to 150 rad/s over 10 seconds, while the load torque fluctuates in both increasing and decreasing phases. These simulations aim to assess the system's ability to maintain optimal performance under sudden changes in both speed and torque demands. The results from the solar PV system, fuel cell, and motor power are also analyzed in this case.

The primary objective of this case is to observe the system's response to rapid changes in both motor speed and load torque. Figure 25 illustrates these variations. The motor speed begins at 100 rad/s and increases steadily to 150 rad/s by 10 seconds. During this time, the load torque follows a dynamic pattern, starting at 50 Nm and rising to 100 Nm at 2.5 seconds, then peaking at 200 Nm by 5 seconds. After this peak, the torque decreases to 180 Nm at 7.5 seconds, and continues to reduce to 150 Nm at 10 seconds. The torque then experiences another decrease to 120 Nm at 12.5 seconds, 70 Nm at 15 seconds, and finally back to 50 Nm at 17.5 seconds.

As the speed increases and the torque fluctuates, the motor must adapt to the rapidly changing load conditions. Under these conditions, the ANN-based Model Predictive Control (MPC) effectively regulates the motor's speed and torque, ensuring smooth transitions and reducing the impact of these fluctuations on the system's performance. The controller predicts the future behavior of the motor and adjusts the input parameters to maintain stability, even during rapid changes. Compared to traditional control methods like PI, ANN MPC provides faster response times and better torque regulation, minimizing disturbances during transitions.

Despite the dynamic changes in speed and load torque, the PV system plays a consistent role in energy generation.

Figure 26 shows the PV cell's output voltage, current, and power under the given conditions. Since the irradiance remains constant, the power generated by the PV array remains stable, providing a steady supply of energy to the system. The PV output is boosted by a Maximum Power Point Tracking (MPPT) algorithm to maintain optimal voltage and power output.

The DC-DC converter further regulates the PV system's voltage, ensuring it provides a steady 400V to the Quadratic Bidirectional Buck-Boost Converter (QBBC) and motor drive. The consistent power output from the PV system helps stabilize the motor's performance, despite the rapid changes in torque and speed demands. The MPPT-operated boost converter ensures that the PV system operates at its maximum efficiency, even as the motor's power requirements fluctuate.

The fuel cell acts as the primary energy source, providing additional power when the PV system alone cannot meet the motor's demands. As shown in Figure 27, the fuel cell's output voltage, current, and power fluctuate depending on the motor's load torque and speed changes. When the motor speed increases and the load torque peaks at 200 Nm, the fuel cell output increases to meet the heightened power demand. Conversely, when the load torque drops, the fuel cell adjusts its output accordingly, ensuring the system operates efficiently.

The fuel cell's converter stabilizes the output voltage, maintaining a constant supply to the motor drive. This ability to dynamically adjust its power output in response to changes in motor load and speed ensures that the system has a reliable and uninterrupted energy source. The fuel cell, combined with the PV array, creates a hybrid system that effectively balances energy generation and consumption, allowing the vehicle to maintain optimal performance even under varying conditions.

The variations in motor speed and load torque have a direct impact on the motor's active and reactive power, as shown in Figure 28. The active power is responsible for the mechanical work performed by the motor, and it increases significantly during the periods when the motor speed and load torque are high. For example, when the torque peaks at 200 Nm, the motor's active power also reaches its maximum, ensuring that sufficient energy is provided to meet the high torque demand.

As the load torque decreases after 10 seconds, the active power correspondingly drops. This reduction reflects the lower energy requirement for the motor to maintain its reduced torque output. The reactive power, which is needed for maintaining the motor's magnetic field, fluctuates in tandem with the active power, but to a lesser extent. The ANN-based MPC helps regulate both active and reactive power more efficiently than traditional control methods, minimizing power losses and ensuring that the motor operates with maximum efficiency during these changing load conditions.

The simulation results in Case 4 highlight the robustness of the proposed electric vehicle configuration, particularly under rapidly changing motor speed and load torque conditions. The ANN-based Model Predictive Control (MPC) demonstrates superior performance in managing these changes, with faster response times and smoother transitions in both speed and torque. The QBBC converter ensures that the motor receives a stable voltage, despite the fluctuations in load conditions, and the combined power from the PV system and fuel cell provides a reliable energy supply throughout the test. Overall, the ANN MPC system offers significant improvements over traditional PI control, providing better stability, efficiency, and responsiveness during dynamic operating conditions. The effective regulation of both active and reactive power further enhances the motor's performance, ensuring that the vehicle operates smoothly even during rapid changes in speed and load torque.

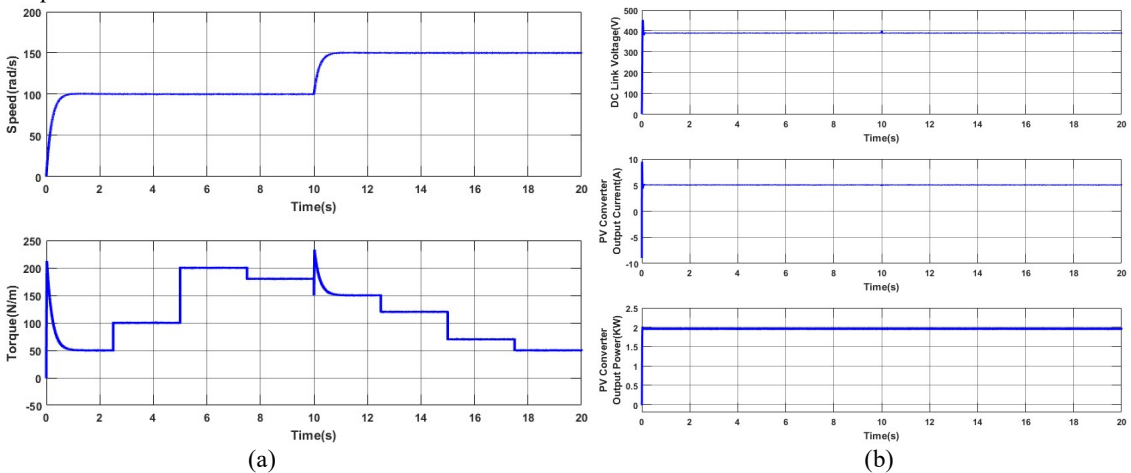


Fig 25. (a) Motor Speed and Torque. (b) PV converter output voltage, current and power

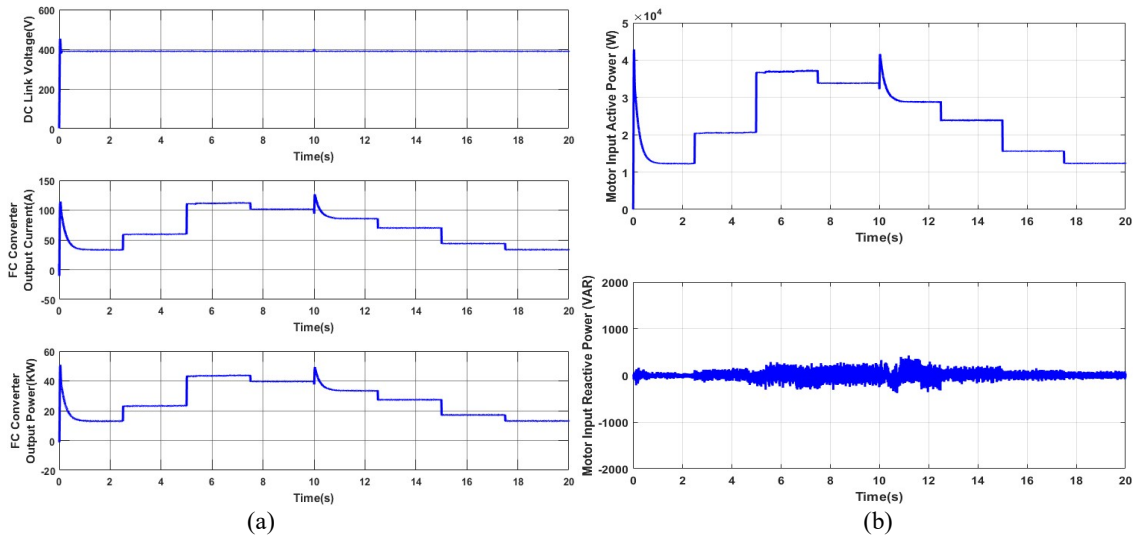


Fig 27. (a) FC converter output voltage, current and power, (b) Motor Input active and reactive power **7. Conclusion**

In this study, a novel electric vehicle (EV) configuration is proposed, integrating multiple energy sources, including a fuel cell, electrolyzer, and onboard photovoltaic (PV) cell. A quadratic bidirectional buck-boost converter is employed to manage the power flow between the motor and energy sources, while an Artificial Neural Network (ANN)-based Model Predictive Control (MPC) system optimizes overall performance. Extensive MATLAB/SIMULINK simulations were conducted to evaluate the system's ability to efficiently manage power generation and consumption under varying irradiance and speed conditions. The inclusion of the PV cell enhances sustainability by reducing dependence on the fuel cell when sufficient solar energy is available. During idle periods, excess PV-generated energy is stored as hydrogen via the electrolyzer, improving energy utilization. The use of an enhanced incremental conductance algorithm for Maximum Power Point Tracking (MPPT) ensures optimal energy capture, even under fluctuating environmental conditions. The ANN-based MPC system demonstrates superior motor control, achieving high accuracy in speed regulation and simplifying the complexity associated with traditional predictive torque control methods. By integrating advanced control strategies with renewable energy sources, this innovative EV configuration shows significant improvements in energy efficiency, system robustness, and sustainability. The study underscores the potential of combining renewable energy technologies with modern control systems to create more efficient and eco-friendly EV designs. Future work will focus on refining control algorithms, increasing scalability, and assessing the system's real-world performance in diverse operational environments.

References

- 1. Elvas, Luis B., and Joao C. Ferreira. "Intelligent transportation systems for electric vehicles." *Energies* 14, no. 17 (2021): 5550.
- 2. Timilsina, L., Badr, P.R., Hoang, P.H., Ozkan, G., Papari, B. and Edrington, C.S., 2023. Battery degradation in electric and hybrid electric vehicles: A survey study. *IEEE Access*, *11*, pp.42431-42462.
- 3. Nouri, Achraf, Aymen Lachheb, and Lilia El Amraoui. "Optimizing efficiency of Vehicle-to-Grid system with intelligent management and ANN-PSO algorithm for battery electric vehicles." *Electric Power Systems Research* 226 (2024): 109936.
- Çimen, Halil, Nurettin Çetinkaya, Juan C. Vasquez, and Josep M. Guerrero. "A microgrid energy management system based on non-intrusive load monitoring via multitask learning." *IEEE Transactions* on Smart Grid 12, no. 2 (2020): 977-987.
- Shi, Gengjin, Miaomiao Ma, Donghai Li, Yanjun Ding, and Kwang Y. Lee. "A process-model-free method for model predictive control via a reference model-based proportional-integral-derivative controller with application to a thermal power plant." Frontiers in Control Engineering 4 (2023): 1185502.

- 6. Babatunde, Damilola Elizabeth, Ambrose Anozie, and James Omoleye. "Artificial neural network and its applications in the energy sector: an overview." *International Journal of Energy Economics and Policy* 10, no. 2 (2020): 250-264.
- Restrepo, Carlos, Catalina Gonzalez-Castano, Javier Munoz, Andrii Chub, Enric Vidal-Idiarte, and Roberto Giral. "An MPPT algorithm for PV systems based on a simplified photo-diode model." *IEEE Access* 9 (2021): 33189-33202.
- 8. Mirzaeva, G. and Mo, Y., 2023. Model predictive control for industrial drive applications. *IEEE Transactions on Industry Applications*.
- 9. Fan, Guangyao, Zhijian Liu, Xuan Liu, Yaxin Shi, Di Wu, Jiacheng Guo, Shicong Zhang, Xinyan Yang, and Yulong Zhang. "Two-layer collaborative optimization for a renewable energy system combining electricity storage, hydrogen storage, and heat storage." *Energy* 259 (2022): 125047.
- 10. He, H., Jia, C. and Li, J., 2022. A new cost-minimizing power-allocating strategy for the hybrid electric bus with fuel cell/battery health-aware control. *International Journal of Hydrogen Energy*, 47(52), pp.22147-22164.
- 11. Sorlei, Ioan-Sorin, Nicu Bizon, Phatiphat Thounthong, Mihai Varlam, Elena Carcadea, Mihai Culcer, Mariana Iliescu, and Mircea Raceanu. "Fuel cell electric vehicles—A brief review of current topologies and energy management strategies." *Energies* 14, no. 1 (2021): 252.
- 12. Khalatbarisoltani, A., Boulon, L. and Hu, X., 2023. Integrating model predictive control with federated reinforcement learning for decentralized energy management of fuel cell vehicles. *IEEE Transactions on Intelligent Transportation Systems*.
- Nguyễn, Bảo-Huy, Thanh Vo-Duy, Carlos Henggeler Antunes, and Joao Pedro F. Trovao. "Multiobjective benchmark for energy management of dual-source electric vehicles: An optimal control approach." *Energy* 223 (2021): 119857.
- 14. Aly, Mokhtar, and Hegazy Rezk. "An improved fuzzy logic control-based MPPT method to enhance the performance of PEM fuel cell system." *Neural Computing and Applications* (2022): 1-12.
- Sun, Haochen, Zhumu Fu, Fazhan Tao, Longlong Zhu, and Pengju Si. "Data-driven reinforcement-learning-based hierarchical energy management strategy for fuel cell/battery/ultracapacitor hybrid electric vehicles." *Journal of Power Sources* 455 (2020): 227964.
- 16. Dao, Hoang Vu, Xuan Dinh To, Hoai Vu Anh Truong, Tri Cuong Do, Cong Minh Ho, Tri Dung Dang, and Kyoung Kwan Ahn. "Optimization-based fuzzy energy management strategy for PEM fuel cell/battery/supercapacitor hybrid construction excavator." *International Journal of Precision Engineering and Manufacturing-Green Technology* 8 (2021): 1267-1285.
- 17. Anbarasu, Arivoli, Truong Quang Dinh, and Somnath Sengupta. "Novel enhancement of energy management in fuel cell hybrid electric vehicle by an advanced dynamic model predictive control." *Energy Conversion and Management* 267 (2022): 115883.
- 18. Ye, Kanglong, and Peiqing Li. "A new adaptive PSO-PID control strategy of hybrid energy storage system for electric vehicles." *Advances in Mechanical Engineering* 12, no. 9 (2020): 1687814020958574.
- 19. Merabet, Ghezlane Halhoul, Mohamed Essaaidi, Mohamed Ben Haddou, Basheer Qolomany, Junaid Qadir, Muhammad Anan, Ala Al-Fuqaha, Mohamed Riduan Abid, and Driss Benhaddou. "Intelligent building control systems for thermal comfort and energy-efficiency: A systematic review of artificial intelligence-assisted techniques." *Renewable and Sustainable Energy Reviews* 144 (2021): 110969.
- Miah, M.S., Hossain Lipu, M.S., Meraj, S.T., Hasan, K., Ansari, S., Jamal, T., Masrur, H., Elavarasan, R.M. and Hussain, A., 2021. Optimized energy management schemes for electric vehicle applications: A bibliometric analysis of future trends. Sustainability, 13(22), p.12800.

- 21. Li, Lin, Tiezhu Zhang, Jichao Hong, Hongxin Zhang, Jian Yang, Zhen Zhang, and Kaiwei Wu. "Energy management strategy of a novel mechanical–electro–hydraulic power coupling electric vehicle under smooth switching conditions." *Energy Reports* 8 (2022): 8002-8016.
- 22. Wang, Tao, Jinyi Wang, Chang Zhang, Pengjie Wang, Zhibo Ren, Haijiao Guo, Zhan Wu, and Fan Wang. "Direct operational data-driven workflow for dynamic voltage prediction of commercial alkaline water electrolyzer based on artificial neural network (ANN)." *Fuel* 376 (2024): 132624.